Integration of wireless power transfer technology with hierarchical multi-walled carbon nanotubes-Polydimethylsiloxane piezo-responsive pressure sensor for remote force measurement

Saman Azhari, Kouki Kimizuka, Gábor Méhes, Yuki Usami, Yasuhiko Hayashi, Hirofumi Tanaka, Takeo Miyake

***Abstract*— Integrating sensory devices with wireless power transfer technology for remote sensing requires the implementation of complex electronic circuitry and communication protocols. To overcome this challenge and remotely monitor mechanical force, we directly integrated piezo-responsive porous multi-walled carbon nanotubes/polydimethylsiloxane nanocomposites with a near-field wireless power transfer system. The wireless system transfers power bidirectionally between the transmitter and the sensing receiver at the resonant frequency of 13.56 MHz. The detection principle is based on the mechanical force-induced impedance changes in the receiver circuit. The modulated impedance signal is detected wirelessly at the transmitter circuit via a full-bridge rectifier and smoothing capacitor. Furthermore, we demonstrate the wireless monitoring of finger bending and applied force using our flexible and disposable sensor without using any energy storage devices. The results suggest a response and recovery time of 400 ± 50 ms, strain sensitivity of 24.73, and pressure sensitivity of 0.98. Our approach adds a new path for disposable haptic-based sensory applications that do not require complex communication protocols in medical, robotics, and other fields.**

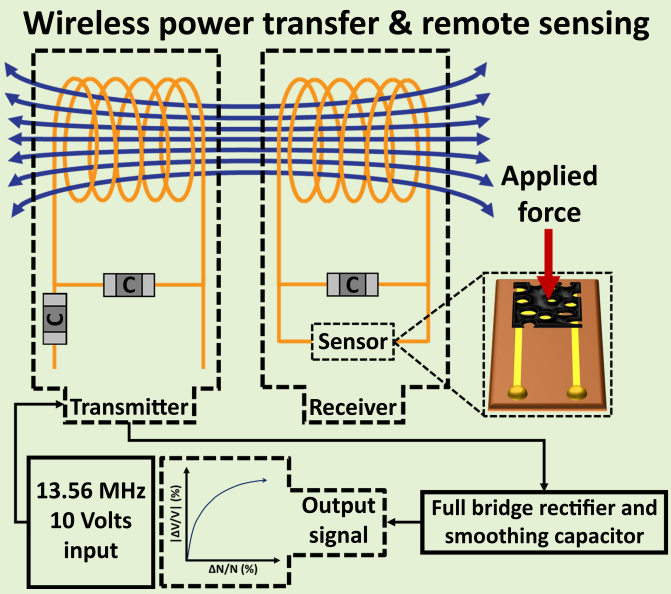

***Index Terms*— CNTs, PDMS, Porous tactile sensor, Wireless power transfer, Remote sensing, Piezo-impedance**

This work was partially supported by JST, SCORE University Promotion Type grant no. JPMJST2053, the CASIO SCIENCE PROMOTION FOUNDATION, the Canon Foundation and ASAHI KOHSAN Company Ltd.

Saman Azhari is with the Waseda University, Graduate School of Information, Production and Systems, 2-7 Hibikino, Wakamatsu-ku, Kitakyushu city 8080135, Japan; he is also a member of the Research Center for Neuromorphic AI Hardware, Kyushu Institute of Technology (Kyutech), Wakamatsu, Kitakyushu 8080196, Japan, (e-mail: saman@aoni.waseda.jp).

Kouki Kimizuka, is with the Kyushu Institute of Technology (Kyutech), Currently pursuing his M.Eng., (e-mail: kimizuka.kouki146@mail.kyutech.jp).

Gábor Méhes, is with the Waseda University, Graduate School of Information, Production and Systems, (e-mail: mehes.gabor@aoni.waseda.jp).

Yuki Usami, is with the Kyushu Institute of Technology (Kyutech); in addition, he is a member of the Research Center for Neuromorphic AI Hardware, Kyushu Institute of Technology (Kyutech), (e-mail: usami@brain.kyutech.ac.jp).

I. Introduction

DUE to their remarkable electrical, mechanical, and chemical properties, functional nanocomposites have applications spanning from textile and food industries through biosensing, energy harvesting, transportation, information technology, and healthcare, making them essential compo-

Yasuhiko Hayashi, is a professor at the Graduate School of Natural Science and Technology, Okayama University, 3-1-1 Tsushimanaka, Kita-ku, Okayama 7008530, Japan, (e-mail: hayashi.yasuhiko@ec.okayama-u.ac.jp).

Hirofumi Tanaka, is with the Kyushu Institute of Technology (Kyutech); in addition, he is a member of the Research Center for Neuromorphic AI Hardware, Kyushu Institute of Technology (Kyutech), (e-mail: tanaka@brain.kyutech.ac.jp).

Takeo Miyake, is with the Waseda University, Graduate School of Information, Production and Systems, (e-mail: miyake@waseda.jp).

nents of future technologies [1]. Since the initial reports of its piezoresistive behavior [2], multi-walled carbon nanotubes (MWCNTs)/polydimethylsiloxane (PDMS) nanocomposites have mainly been investigated for flexible electronics and piezoresistive pressure sensing applications. While there have been significant improvements and achievements regarding piezoresistive MWCNTs/PDMS nanocomposites that enhance their sensitivity, detection limit, and stability mainly via hierarchical structure and increased porosity [3]–[6], there are significant drawbacks in MWCNTs/PDMS sensor fabrication. An example of such drawbacks is the attachment of the sensor to electrodes. Most reports that investigate the piezoresistive effects of MWCNTs/PDMS insufficiently address this problem. Typically, researchers use silver epoxy or copper tapes as conductive adhesives, which are not viable options, particularly for commercial applications, due to high contact resistance and low mechanical integrity.

Recently, the use of silane bonding of PDMS with various materials and surfaces has been investigated. The reports show good mechanical properties, particularly for flexible devices and applications [7]–[10]. In addition, reports on high-frequency applications of MWCNTs/PDMS, particularly piezo-impedance sensing [11], [12], suggest that at high frequencies (>100 KHz), MWCNTs/PDMS exhibit a robust capacitive response, while at low frequencies (<100 KHz), the resistive response is dominant. Moreover, porous MWCNTs/PDMS, fabricated via sacrificial template, have been shown to have high capacitive sensitivity at high frequencies. This behavior has been correlated with capacitance forming between carbon nanotubes (CNTs)-PDMS-CNTs structure and resistive-capacitive (RC) network forming at CNTs-CNTs junctions [12]. This multimodal behavior makes MWCNTs/PDMS an exciting material for high-frequency applications.

Resonant inductive coupling (magnetic resonance coupling), particularly at 13.56 MHz, for near-field power transmission as a high-frequency application, is one of the main routes to wireless power transmission (WPT) technologies [13], [14]. WPT and remote sensing (RS) are rapidly becoming essential technologies of modern electronics and sensory devices [15], [16]. Although wirelessly powered wearable electronics have been investigated extensively [17]–[19], their integration with RS technology requires complex circuitry [20]–[22].

The current trend in integrating WPT with wearable electronics is mainly focused on power transmission [23]. For example, there are multiple reports on using WPT technology to power up a component on the receiver via AC to DC conversion [18], [19]. Some of these works report the evidence of change in the receiver impedance (Z_R) [17]–[19] upon physical changes or chemical reactions having influenced a passive component of the receiver circuit [17], [18]. Due to coupling between the transmitter and receiver circuits, these changes affect multiple parameters, resulting in the detection of Z_R variation via the transmitter. Therefore, even though there are reports on the integration of WPT with complex and costly data communication protocols and devices [15], [16], [24]–[26], the presence of multiple coupling-induced parameters in WPT systems that are affected by Z_R suggests the prospect of RS based on simply detecting changes in Z_R without the necessity for additional communication protocols and complex circuitry.

The use of piezo-responsive MWCNTs/PDMS nanocomposite as a remote wearable device has yet to be fully realized. Herein, the challenges outlined above are addressed by presenting a chemically bonded porous MWCNTs/PDMS nanocomposite sensor fabricated via the sacrificial template technique on screen-printed interdigitated (IDT) electrodes with reduced contact resistance. Wirelessly powering the nanocomposite sensor without additional rectification or power storage units enables the remote monitoring of the applied force on the piezo-responsive nanocomposite using its high-frequency characteristics and reflected impedance. The direct integration of high-frequency piezo-responsive MWCNTs/PDMS nanocomposite with near-field (13.56 MHz) WPT technology and a simple readout circuit (a full bridge rectifier and a filter) simplifies the measurement system and improves cost-effectiveness. We expect our technology to accelerate the development of disposable wirelessly powered remote pressure sensing devices, not requiring complicated circuitry and communication protocols.

II. Experimental

A. Materials

Multi-walled carbon nanotube (MWCNT) provided by Cnano Technology (FT9110; Santa Clara, CA, USA), polydimethylsiloxane (PDMS) (Sylgard 184, Dow Corning), commercially available household white sugar, D-550 silver ink (DOTITE), 99% (3-Aminopropyl)triethoxysilane (APTES) (Sigma Aldrich) and 50 μm thick Kapton film (As One) were purchased and used at it is. AWG 31 wire was used for the antenna fabrication.

B. Fabrication of transmitter, receiver, and remote sensing circuit

The transmitter and receiver antennas were designed and fabricated based on a previously published work [18]. In short, a five-turn copper wire coil (wire diameter: 0.238 mm and coil diameter: 35 mm) covered with heat-shrink tubing was attached to chip capacitors by tinning with a soldering iron. The transmitter resonance frequency was tuned to 13.56 MHz $\pm$ 200 KHz by attaching a 42 pF capacitor in parallel and a 42 pF capacitor in series, while the receiver was tuned to the same resonance frequency by attaching an 80 pF capacitor in parallel. The values for tuning capacitors were determined via a vector network analyzer (VNA) (Anritsu-MS46122B) so that both antennas would have near zero Imaginary impedance (Im[Z]) at the resonance frequency. For remote sensing (RS), the input of the transmitter coil was connected to a full bridge rectifier (FBR) assembled using 1N4448 diodes. The output of the FBR was connected to a 2 mF smoothing capacitor ($C_{smoothing}$) connected in parallel to a 100 Ω resistor (R_{out}), as shown in Figure S1.

C. Fabrication of CNTs/PDMS sensor

PDMS prepolymer was prepared by mixing 30 grams of base and 3 grams of curing agent, vigorously stirred for 20 minutes, covered to avoid contamination, and kept in the freezer (-12.5 °C) for degassing. 0.2 grams of MWCNTs were directly mixed with 20 grams of sugar using a pestle, and mortar [27]. The resulting mixture was wetted with 600 μL water and molded into a 5 × 5 × 0.2 cm cuboid. After drying the sample in the oven at 70 °C for 6 hours, the MWCNTs-sugar cuboid was demolded and placed in a Petri dish filled with previously prepared PDMS prepolymer. The Petri dish was placed in a vacuum desiccator for 1 hour, then covered to avoid contamination, and placed in the freezer at -12.4 °C for an additional hour. This process resulted in PDMS infusion in MWCNTs-sugar pores due to the capillary effect caused by vacuum and shrinkage. The MWCNTs-sugar-PDMS cuboid was taken out, excess PDMS prepolymer on the surface was wiped off and then placed in the oven at 70 °C for 24 hours for the curing process. After curing, sandpaper was used to polish and smoothen the sample's surface. The sample was placed into a beaker filled with distilled water and heated in a conventional microwave oven for 5 minutes to dissolve the sugar. Microwave heating expedites sugar dissolution due to the expansion of pores as a result of thermal shock [28]. The dissolution of sugar in the water changes the color of the water to brown. The water was discarded after each cycle. This process was repeated five or more times until the water remained clear. The final product was then dried for 1 hour at 125 °C and cut into 1 × 1 × 0.2 cm cuboids (Figure S2).

Sensors were fabricated by attaching MWCNTs/PDMS nanocomposite to screen-printed IDT silver electrodes on a Kapton film. Silane coupling [29], [30] using 1 vol% aqueous APTES was employed to reduce the effects of contact resistance and improve the mechanical integrity of attachment. Silane coupling was performed by placing the electrodes and the MWCNTs/PDMS in UV ozone cleaner for 30 minutes and then immersing the electrodes in 1 vol% aqueous APTES for 30 minutes at room temperature for surface functionalization. Lastly, MWCNTs/PDMS nanocomposite was placed on top of the electrode, clamped tightly, and placed in the oven at 70 °C for 1 hour (Figure S3) to obtain the sensing device.

D. Measurement

Initially, the transmitter and receiver were tuned to the resonance frequency by soldering each antenna to the SMA connector (Orient Microwave BL52-5636-00), connecting them to VNA (Anritsu-MS46122B), measuring the impedance at 13.56 MHz, and using the Smith chart impedance matching technique to determine the value of the ideal capacitors (as mentioned in section 2.2). After tuning, the scattering parameters (S-parameter) were determined via the same setup.

To characterize the hierarchical structure of MWCNTs/PDMS nanocomposite, scanning electron microscopy (JEOL, JCM-7000 NeoScope) was utilized. The contact resistance of two sensors, one with silver paste and another with APTES as their bonding agent, was determined using an impedance analyzer (HIOKI IM 3570). The piezo-impedance performance of MWCNTs/PDMS was evaluated by collecting the impedance and phase angle from 5 MHz to 1 KHz using an impedance analyzer (HIOKI IM 3570) while measuring the force using IMADA digital force gauge (ZTS-5N) and displacement via Mitutoyo micrometer simultaneously (all connected to PC via Universal Serial Bus), as shown in Figure S4. For RS measurements, the transmitter input was connected to a function generator (200 MHz NF corporation multifunction generator WF1968), while the receiver was connected to the fabricated sensor in parallel. The voltage drop across R_{out} was measured via Arduino Uno (Arduino) connected to PC via Universal Serial Bus (Figure S1). The data were collected using MATLAB (MathWorks), Labview 2021 (National Instruments), and Force logger (Software provided by IMADA Corp), while the plots were graphed via Origin Pro 2022 (OriginLab Corporation).

III. Results and discussion

A. Hierarchical structure and contact resistance

The formation of a hierarchical structure has been shown to improve the piezo properties of MWCNTs/PDMS [3]–[6]. The result shown in Figure S5, obtained via scanning electron microscopy imaging, confirms the porous hierarchical structure of MWCNTs/PDMS nanocomposite. The pore size of the nanocomposite, created by the removal of sugar particles, has an average diameter of 235 µm ± 134 µm, which is in the range of sugar particle size. The formation of these hierarchical structures improves the flexibility, thereby increasing the sensitivity and stability of the MWCNTs/PDMS piezoresistive nanocomposite [3]–[6]. In addition, the contact resistance between the screen-printed IDT silver electrodes and the MWCNTs/PDMS decreased using APTES as a silane coupling agent compared to using the silver paste. The results shown in Figure S6 indicate that the contact resistance has significantly declined from 4.2 KΩ in the sample with Ag paste as the adhesive to 2.73 KΩ in the sample with APTES as the silane coupling agent. These results confirm the attachment of hierarchical MWCNTs/PDMS structure to screen-printed IDT silver electrode with reduced contact resistance [31].

B. Piezo response characterization of sensor

Since the piezo characteristics of the porous hierarchal MWCNTs/PDMS nanocomposite sensor are crucial to the purpose of this study, we evaluated the nanocomposite's flexibility, piezo-response, and sensitivity for wearable applications. The sensor retains its elasticity in the target pressure range (up to 5 N), as shown in Figure 1a. The exponential tendency with a growth constant of k = 0.02 and time constant τ = 49.22 indicates that the increased compression increases the Young's modulus of the sample. This is understood because the initial applied force compresses the pores, resulting in a rapid change in strain and filling the voids in the porous structure of the MWCNTs/PDMS nanocomposite. As a result, the deformation rate of the MWCNTs/PDMS sensor decreases with the compression force. The hysteresis of 5.8 % observed in Figure 1a inset is due to the elastomeric nature of the matrix material (PDMS), often seen in PDMS-based pressure

sensors [32], [33]. To evaluate the piezo-impedance response of the device, we plot the Nyquist and Bode phase plots of the sensor, as shown in Figures 1b and 1c, respectively. Figure 1b indicates the decrease in both the real and imaginary axes due to applied force [12]. When force is exerted on the MWCNTs/PDMS sensor while measuring its impedance at high frequencies (>100 KHz), the capacitance value increases while the resistance value decreases; this is further evident in Figure 1c. Based on these data, we can conclude that the impedance response of the device with respect to applied force varies at high and low frequencies with the gauge factor of 0.68 at 5 MHz determined using equation 1.

$$GF = \frac{\Delta Z/Z_o}{\Delta L/L_0} = \frac{\Delta Z/Z_0}{\varepsilon} \tag{1}$$

In contrast, the shift in the phase angle is observed only at high frequencies with the slope of 1.8 at 5 MHz. Furthermore, Figures 1b and 1c reveal that the phase angle above 1.5 N shifts towards the positive region (Inductive), suggesting that due to applied force, the device begins to behave as a conductor, resulting in a positive phase angle. Finally, and importantly, the apparent shift in the phase angle at high frequencies due to the applied force reveals the possible application of MWCNTs/PDMS sensors for high-frequency applications. WPT technology based on inductive coupling is in the MHz range, which makes it suitable for MWCNTs/PDMS piezo-responsive applications.

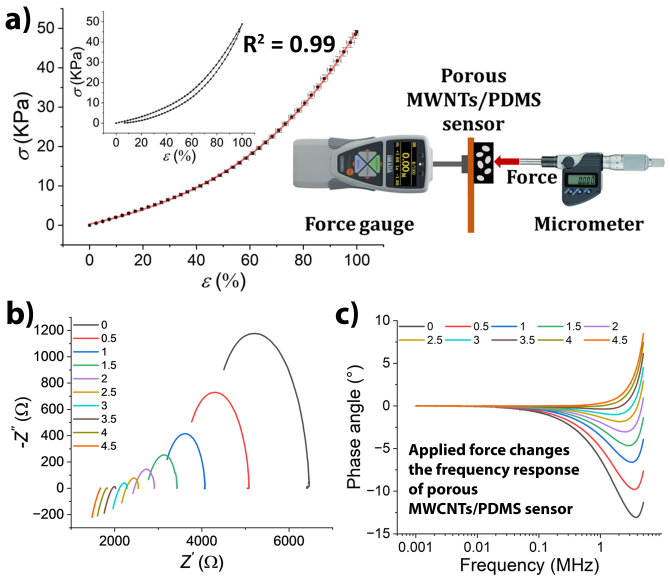

Fig. 1. a) Data (black dots) and fitted curve (red line) correspond to the stress vs. strain and schematic of measurements setup (The inset corresponds to the cyclic measurement). The error bars represent the standard deviation of 3 consecutive measurements from the same sample. b) Nyquist and c) Bode phase plots, obtained from porous MWCNTs/PDMS nanocomposite under an applied force of 0 N – 4.5 N with intervals of 0.5 N.

C. Characterization of WPT efficiency and influence of coupling on remote sensing

An important parameter in the WPT system is the wireless power transfer efficiency (η) that varies with the radiation distance (air gap between transmitter and receiver). In a two-port network, η, shown in equation 2, was determined by varying the distance between transmitter and receiver antennas tuned at the resonance frequency (13.56 MHz), where P_{in} and P_{out} are transmitter power and receiver power, respectively. Equations 3 and 4 relate η to the scattering parameter (S_{21}) that signifies the power that leaves port 1 (Transmitter) and enters port 2 (Receiver).

$$\eta = \frac{P_{out}}{P_{in}} \tag{2}$$

$$S_{21} = 10log\frac{P_{out}}{P_{in}} \tag{3}$$

$$\eta = 10^{\frac{S_{21}}{10}} \tag{4}$$

η is in inverse correlation with radiation distance [17], [18]. The correlation between η and the radiation distance in simple coil loop antennas used in this work was determined by the Boltzmann function, shown in equation 5.

$$\eta = \frac{Initialvalue - Final\ value}{1 + e^{\frac{Distance - Center}{Slope}}} + Final\ value \tag{5}$$

The results shown in Figure 2a indicate the η = 5.88 % at 0.5 cm and η = 0.18 % at 4 cm radiation distance with the slope of 0.62, which signifies the inverse correlation between η and the radiation distance. This tendency is reported in previous works and is due to the change in coupling coefficient (k) and mutual inductance, determined by equation 6, and $L_m = k\sqrt{L_T L_R}$, respectively, where d is the radiation distance, r_1 and r_2 are the radii of transmitter and receiver antennas (17.5 mm), L_T and L_R are transmitter (6.56 μH) and receiver (1.72 μH) inductance, respectively [18].

$$k = \frac{1}{\left[1 + 2^{\frac{2}{3}}\left(d/\sqrt{r_1 r_2}\right)^2\right]^{\frac{3}{2}}} \tag{6}$$

To confirm the initial hypothesis regarding the possibility of remotely monitoring the change in resistance of porous MWCNTs/PDMS nanocomposite, the S_{11} parameter was recorded at a 1 cm gap between the transmitter and receiver. This distance was selected to avoid over coupling due to proximity but also low WPT efficiency at higher radiation distances. S_{11} has a linear correlation with applied pressure [26] with a slope value of 0.3, as shown in Figure 2c. In addition, η decreases exponentially (Eq. 7) with a decay constant of k = -0.28 and time constant of τ = -3.57 as the applied pressure increases (Figure 2d), indicating that the change in Z_R influences the WPT efficiency and the S-parameters. The observed trends indicate a direct and measurable influence of the changes in receiver impedance on the electrical behavior of the transmitter as a result of applied force on the piezo-responsive sensor.

$$\eta = Offset + Amplitude \times e^{\frac{-Force}{Time\ constant}} \tag{7}$$

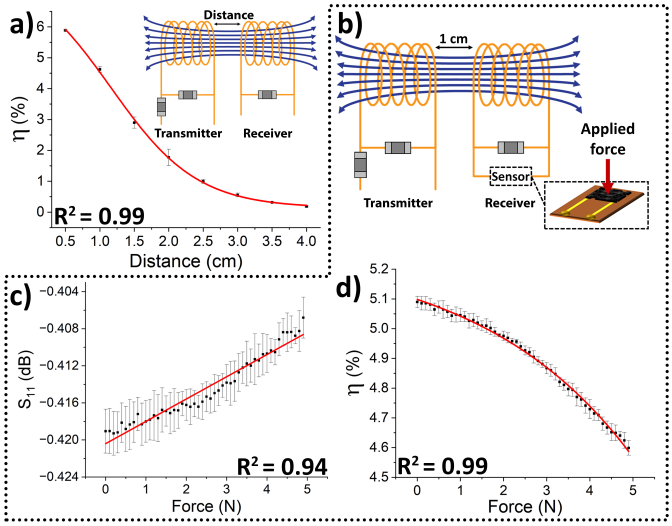

Fig. 2. The data (black dots) and fitted curve (red line) correspond to a) power transfer efficiency vs. radiation distance between transmitter and receiver antennas (inset shows the schematic of the measurement). b) schematic of WPT characterization in correlation with applied force on the porous piezoresistive MWCNTs/PDMS sensor via VNA and the corresponding c) S_{11} parameter and d) power transfer efficiency. The error bars represent the standard deviation of 3 consecutive measurements from the same sample.

D. Performance of WPT remote sensing system

The circuit shown in Figure S1 was constructed to measure the changes in receiver impedance via the transmitter. The RS capability of the sensor at a radiation distance of 1 cm was recorded in real-time using Arduino Uno. Based on the results shown in Figure 3a, during the RS measurements, the output voltage varies because of deformation. The change in output voltage in response to deformation (ε) is fitted using the Boltzmann function as shown in equation 8, indicating that the voltage changes rapidly (Slope = 24.73) as it gets closer to the center (ε = 66.84 %), and begins to slow down while reaching the final value.

$$|\frac{\Delta V}{V}| = \frac{Initial\ value - Final\ value}{1 + e^{\frac{\varepsilon - Center}{Slope}}} + Final\ value \quad (8)$$

This data shows that the change in output voltage at low and high deformation states is small, while it is rapid in the mid-range with the center at ε = 66.84 %. As shown in Figure 3b, the change in output voltage in response to applied force was fitted using the asymptote fitting function shown in equation 9, indicating a rapid change in the initial stages and slowing down near saturation (Rate = 0.98). These data suggest that the fabricated sensor has potential as a midrange strain gauge and low-pressure range piezoresistive pressure sensor for accurately monitoring different states and conditions of a system remotely.

$$|\frac{\Delta V}{V}| = Asymptote - Response\ range \times Rate^{\frac{\Delta N}{N}} \quad (9)$$

To confirm the functionality and applicability of the proposed system, the sensor was attached to a nitrile glove on the palmar side of the index finger at the proximal interphalangeal (PIP) joint using a double-sided tape and connected to the setup shown in Figure S1. The real-time recording of the sensor during repeated bending to 45 ° (0.05 N) or 90 ° (0.1 N) and flexing of the hand (0 N) shows the doubling of the output voltage drop from 45 mV to 90 mV with the response and recovery time of 400 ± 50 ms in both cases (Figures 3c and 3d). We note that the modest change in the shape of the response in Figures 3c and 3d is due to the variation in the bending speed of the finger. Furthermore, we tested the functionality of the sensor by applying pressure via fingertip at a 1 cm radiation distance and observed an average voltage drop of 50 mV with a response and recovery time of 400 ± 50 ms (Figure S7). Lastly, the standard weights of 0.5 N, 1 N, and 2 N were applied to the sensor at radiation distances of 1 cm – 4 cm with intervals of 1 cm (Figure S8), which showed the decline in the output voltage, response and recovery time as radiation distance increases. These results demonstrate the high sensitivity, functionality, and applicability of the proposed design in combination with WPT and RS technologies for real-life scenarios.

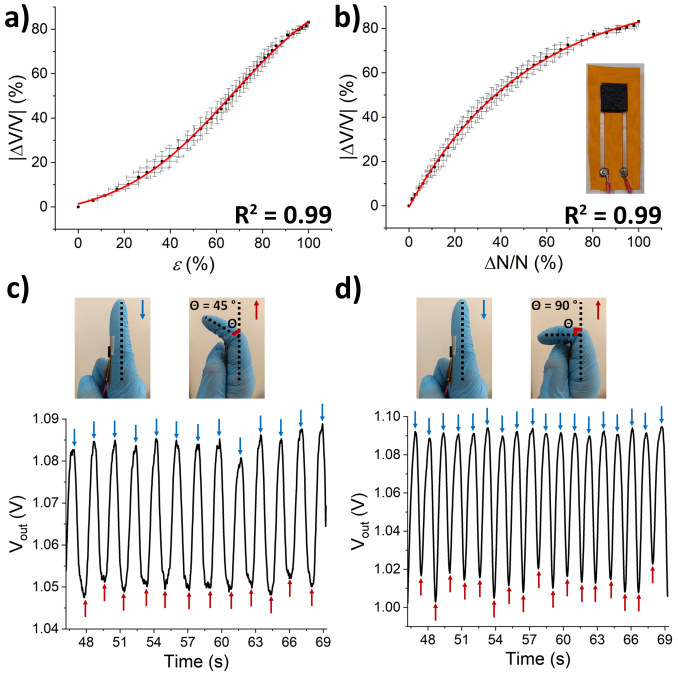

Fig. 3. Output voltage variation of the proposed system with respect to a) sensor deformation (strain) and b) change in applied force (Inset is the closeup image of the sensor). The error bars represent the standard deviation of 3 consecutive measurements from the same sample. The output voltage of the proposed system for c) a 45 ° bending and d) a 90 ° bending.

E. Discussion

From these observations, we infer that during the initial state (no force or deformation), the sensor impedance is high, which then changes with applied force due to the increase in conductive junctions and proximity of MWCNTs in the MWCNTs-PDMS-MWCNTs network. Due to the coupling, these changes affect multiple parameters, resulting in the feasible detection of changes in the receiver through the transmitter.

The value for Z_R is determined using equation 10 where Z_L is inductive, Z_C is capacitive, and Z_S is the sensor impedance value (Figure S9) [17]–[19].

$$Z_R = \frac{1}{\frac{1}{Z_L} + \frac{1}{Z_C} + \frac{1}{Z_S}} \tag{10}$$

Any changes in Z_L, Z_C, or Z_S affect Z_R. During inductive coupling, the changes in Z_R influence the transmitter by altering the reflected impedance (Z'_R). Z'_R is a physical quantity arising from the phenomenon that is directly correlated to the mutual inductance (L_m) between transmitter and receiver. In the WPT system, the input voltage (V_{in}) results in current flow (I_1) in a wire loop of the transmitter, and a magnetic field is generated based on Ampère's Law, which then induces an electromotive force (EMF) in the receiver due to Faraday's Law ($V_{Lm2} = j\omega L_m I_1$). The V_{Lm2} then generates a current (I_2) which induces EMF in the transmitter ($V_{Lm1} = j\omega L_m I_2$). The V_{Lm1} can be perceived as a voltage drop in the transmitter, and Z'_R can be determined based on (Eq. 11).

$$Z'_R = \frac{V_{Lm1}}{I_1} = \frac{j\omega L_m I_2}{I_1} = \frac{(\omega L_m)^2}{Z_R} \tag{11}$$

Due to the piezo-response of the MWCNTs/PDMS sensor, the reflected impedance and hence the resonant inductive coupling are affected. This is because the sensor impedance is initially high, resulting in a higher Z_R, a lower I_2, and the resulting Z'_R. Therefore, the I_1 increases, resulting in the rise in V_{Lm2} and I_2. This leads to a higher voltage drop across the transmitter because V_{Lm1} is linearly correlated to I_2. As the applied force on the sensor increases, the sensor impedance decreases, resulting in lower Z_R, higher I_2, and subsequent Z'_R. Z'_R increases, the I_1 decrease; thus, V_{Lm2} and I_2 drop, which result in lower V_{Lm1}. This can be validated via resonance inductive coupling efficiency (η). At the initial state, when the sensor impedance is high, the η is high, suggesting higher V_{Lm2} and I_2. Applying pressure on the MWCNTs/PDMS then decreases Z_R, which weakens the resonance inductive coupling efficiency (low η) due to the decrease in V_{Lm2} and I_2.

Moreover, the variation in voltage drop across R_{out} (Figures 3c and 3d) and the rise in the S_{11} parameter (Figure 2c) due to applied force is in line with this analogy. These results confirm the possibility of using the fundamental properties of MWCNTs/PDMS nanocomposite and resonance inductive coupling for direct and high-frequency integration of WPT and MWCNTs/PDMS piezo-responsive sensors to monitor the changes in the receiver remotely. Our WPT nanocomposite sensing platform opens up the possibility of using near-field WPT in low-cost applications that do not require complex communication protocols, constant power supply, and continuous measurement, which are easily disposable. Such devices could be used to monitor vital organs' conditions remotely without using energy storage devices that often contain poisonous materials. The application of such a system is not limited to medicine and could be beneficial to the industry (for example, remotely monitoring the state of a device without wasting energy) or machine learning in combination with robotics [34].

IV. Conclusion

In this work, we demonstrated the direct integration of piezo-responsive MWCNTs/PDMS nanocomposite with WPT for RS application using resonant inductive coupling, a full-bridge rectifier, and a smoothing capacitor. Furthermore, we confirmed the stability of piezo-responsive porous MWCNTs/PDMS nanocomposite chemically bonded to the silver electrode using a silane coupling agent with 5.8 % mechanical hysteresis. In addition, we demonstrated the proposed setup's performance with a strain sensitivity of 24.73 and a pressure sensitivity of 0.98. We also mention that while in this first demonstration, the correlation between the efficiency of WPT and the distance between transmitter and receiver and between the efficiency and the magnitude of applied force appears to be limited, a more efficient antenna design is expected to improve such properties. Moreover, the RS performance was assessed by applying force directly to the sensor with a fingertip and attaching the sensor to the PIP joint of a finger while measuring the applied force and bending angle in real-time with high accuracy and fast response. Finally, we showed the correlation of radiation distance with sensor response by applying constant force at various radiation distances. This approach may open a path for disposable medical and other haptic-based applications that do not require complex communication protocols. By miniaturizing the receiver coil and utilizing the proposed setup in the future, we may fabricate a disposable device that can monitor the functions of vital organs on demand and remotely while eliminating the use of energy storage devices.

Acknowledgment

This work was partially supported by JST, SCORE University Promotion Type grant no. JPMJST2053, the CASIO SCIENCE PROMOTION FOUNDATION, the Canon Foundation, and ASAHI KOHSAN Company Ltd.

References

[1] T. Hassan, A. Salam, A. Khan, S. U. Khan, H. Khanzada, M. Wasim, M. Q. Khan, and I. S. Kim, "Functional nanocomposites and their potential applications: A review," *Journal of Polymer Research*, vol. 28, pp. 1–22, 2021.

[2] J. Lu, M. Lu, A. Bermak, and Y.-K. Lee, "Study of piezoresistance effect of carbon nanotube-pdms composite materials for nanosensors," in *2007 7th IEEE Conference on Nanotechnology (IEEE NANO)*, pp. 1240–1243, IEEE, 2007.

[3] X. Sun, J. Sun, T. Li, S. Zheng, C. Wang, W. Tan, J. Zhang, C. Liu, T. Ma, Z. Qi, *et al.*, "Flexible tactile electronic skin sensor with 3d force detection based on porous cnts/pdms nanocomposites," *Nano-micro letters*, vol. 11, pp. 1–14, 2019.

[4] T. R. Michel, M. J. Capasso, M. E. Cavusoglu, J. Decker, D. Zeppilli, C. Zhu, S. Bakrania, J. A. Kadlowec, and W. Xue, "Evaluation of porous polydimethylsiloxane/carbon nanotubes (pdms/cnts) nanocomposites as piezoresistive sensor materials," *Microsystem Technologies*, vol. 26, pp. 1101–1112, 2020.

[5] X. Lei, L. Ma, Y. Li, Y. Cheng, G. J. Cheng, and F. Liu, "Highly sensitive and wide-range flexible pressure sensor based on carbon nanotubes-coated polydimethylsiloxane foam," *Materials Letters*, vol. 308, p. 131151, 2022.

[6] Y. Zhao, T. Shen, M. Zhang, R. Yin, Y. Zheng, H. Liu, H. Sun, C. Liu, and C. Shen, "Advancing the pressure sensing performance of conductive cnt/pdms composite film by constructing a hierarchical-structured surface," *Nano Materials Science*, 2022.

[7] K. Aran, L. A. Sasso, N. Kamdar, and J. D. Zahn, "Irreversible, direct bonding of nanoporous polymer membranes to pdms or glass microdevices," *Lab on a Chip*, vol. 10, no. 5, pp. 548–552, 2010.

[8] M. Agostini, G. Greco, and M. Cecchini, "Polydimethylsiloxane (pdms) irreversible bonding to untreated plastics and metals for microfluidics applications," *APL Materials*, vol. 7, no. 8, p. 081108, 2019.

[9] N. Y. Lee and B. H. Chung, "Novel poly (dimethylsiloxane) bonding strategy via room temperature "chemical gluing"," *Langmuir*, vol. 25, no. 6, pp. 3861–3866, 2009.

[10] K. Kim, S. W. Park, and S. S. Yang, "The optimization of pdms-pmma bonding process using silane primer," *BioChip Journal*, vol. 4, pp. 148–154, 2010.

[11] L. Helseth, "Electrical impedance spectroscopy of multiwall carbon nanotube–pdms composites under compression," *Materials Research Express*, vol. 5, no. 10, p. 105002, 2018.

[12] D.-Y. Jeon, H. Kim, M. W. Lee, S. J. Park, and G.-T. Kim, "Piezo-impedance response of carbon nanotube/polydimethylsiloxane nanocomposites," *APL Materials*, vol. 7, no. 4, p. 041118, 2019.

[13] B. Zhan, W. Xia, C. Xiong, and S. Liu, "Simulation analysis of coupling coil of 13.56 mhz magnetic coupling resonant wireless energy transmission system," in *2021 22nd International Conference on Electronic Packaging Technology (ICEPT)*, pp. 1–6, IEEE, 2021.

[14] E. M. Ali, M. Alibakhshikenari, B. S. Virdee, M. Soruri, and E. Limiti, "Efficient wireless power transfer via magnetic resonance coupling using automated impedance matching circuit," *Electronics*, vol. 10, no. 22, p. 2779, 2021.

[15] R. La Rosa, P. Livreri, C. Trigona, L. Di Donato, and G. Sorbello, "Strategies and techniques for powering wireless sensor nodes through energy harvesting and wireless power transfer," *Sensors*, vol. 19, no. 12, p. 2660, 2019.

[16] S. A. Huda, M. Y. Arafat, and S. Moh, "Wireless power transfer in wirelessly powered sensor networks: A review of recent progress," *Sensors*, vol. 22, no. 8, p. 2952, 2022.

[17] T. Takamatsu, Y. Sijie, F. Shujie, L. Xiaohan, and T. Miyake, "Multifunctional high-power sources for smart contact lenses," *Advanced Functional Materials*, vol. 30, no. 29, p. 1906225, 2020.

[18] T. Takamatsu, Y. Chen, T. Yoshimasu, M. Nishizawa, and T. Miyake, "Highly efficient, flexible wireless-powered circuit printed on a moist, soft contact lens," *Advanced Materials Technologies*, vol. 4, no. 5, p. 1800671, 2019.

[19] H. E. Lee, D. Lee, T.-I. Lee, J. H. Shin, G.-M. Choi, C. Kim, S. H. Lee, J. H. Lee, Y. H. Kim, S.-M. Kang, *et al.*, "Wireless powered wearable micro light-emitting diodes," *Nano Energy*, vol. 55, pp. 454–462, 2019.

[20] J. Kim, A. Banks, Z. Xie, S. Y. Heo, P. Gutruf, J. W. Lee, S. Xu, K.-I. Jang, F. Liu, G. Brown, *et al.*, "Miniaturized flexible electronic systems with wireless power and near-field communication capabilities," *Advanced Functional Materials*, vol. 25, no. 30, pp. 4761–4767, 2015.

[21] J. Kim, G. A. Salvatore, H. Araki, A. M. Chiarelli, Z. Xie, A. Banks, X. Sheng, Y. Liu, J. W. Lee, K.-I. Jang, *et al.*, "Battery-free, stretchable optoelectronic systems for wireless optical characterization of the skin," *Science advances*, vol. 2, no. 8, p. e1600418, 2016.

[22] S.-W. Kim, Y. Lee, J. Park, S. Kim, H. Chae, H. Ko, and J. J. Kim, "A triple-mode flexible e-skin sensor interface for multi-purpose wearable applications," *Sensors*, vol. 18, no. 1, p. 78, 2017.

[23] S. Hui, "Planar wireless charging technology for portable electronic products and qi," *Proceedings of the IEEE*, vol. 101, no. 6, pp. 1290–1301, 2013.

[24] D. Niyato, D. I. Kim, M. Maso, and Z. Han, "Wireless powered communication networks: Research directions and technological approaches," *IEEE Wireless Communications*, vol. 24, no. 6, pp. 88–97, 2017.

[25] H. Kou, L. Zhang, Q. Tan, G. Liu, H. Dong, W. Zhang, and J. Xiong, "Wireless wide-range pressure sensor based on graphene/pdms sponge for tactile monitoring," *Scientific reports*, vol. 9, no. 1, p. 3916, 2019.

[26] B. Xu, M. Li, M. Li, H. Fang, Y. Wang, X. Sun, Q. Guo, Z. Wang, Y. Liu, and D. Chen, "Radio frequency resonator-based flexible wireless pressure sensor with mwcnt-pdms bilayer microstructure," *Micromachines*, vol. 13, no. 3, p. 404, 2022.

[27] Y. Jung, K. K. Jung, D. H. Kim, D. H. Kwak, and J. S. Ko, "Linearly sensitive and flexible pressure sensor based on porous carbon nanotube/polydimethylsiloxane composite structure," *Polymers*, vol. 12, no. 7, p. 1499, 2020.

[28] B. Herren, V. Webster, E. Davidson, M. C. Saha, M. C. Altan, and Y. Liu, "Pdms sponges with embedded carbon nanotubes as piezoresistive sensors for human motion detection," *Nanomaterials*, vol. 11, no. 7, p. 1740, 2021.

[29] V. Sunkara, D.-K. Park, and Y.-K. Cho, "Versatile method for bonding hard and soft materials," *Rsc Advances*, vol. 2, no. 24, pp. 9066–9070, 2012.

[30] V. Sunkara, D.-K. Park, H. Hwang, R. Chantiwas, S. A. Soper, and Y.-K. Cho, "Simple room temperature bonding of thermoplastics and poly (dimethylsiloxane)," *Lab on a Chip*, vol. 11, no. 5, pp. 962–965, 2011.

[31] P. Vadhva, J. Hu, M. J. Johnson, R. Stocker, M. Braglia, D. J. Brett, and A. J. Rettie, "Electrochemical impedance spectroscopy for all-solid-state batteries: Theory, methods and future outlook," *ChemElectroChem*, vol. 8, no. 11, pp. 1930–1947, 2021.

[32] M. O. Tas, M. A. Baker, M. G. Masteghin, J. Bentz, K. Boxshall, and V. Stolojan, "Highly stretchable, directionally oriented carbon nanotube/pdms conductive films with enhanced sensitivity as wearable strain sensors," *ACS Applied Materials & Interfaces*, vol. 11, no. 43, pp. 39560–39573, 2019.

[33] C.-X. Liu and J.-W. Choi, "Strain-dependent resistance of pdms and carbon nanotubes composite microstructures," *IEEE transactions on Nanotechnology*, vol. 9, no. 5, pp. 590–595, 2010.

[34] S. Azhari, T. Setoguchi, I. Sasaki, A. Nakagawa, K. Ikeda, A. Azhari, I. H. Hasan, M. N. Hamidon, N. Fukunaga, T. Shibata, *et al.*, "Toward automated tomato harvesting system: Integration of haptic based piezoresistive nanocomposite and machine learning," *IEEE Sensors Journal*, vol. 21, no. 24, pp. 27810–27817, 2021.

Saman Azhari Saman Azhari received B.Eng (electrical and electronics) from UCSI university in 2012; he then realized a growing interest in material science, particularly nanomaterials and their applications, which led him to persuade his M.Sc the Ph.D. in nanotechnology from Universiti Putra Malaysia in 2016 and 2020, respectively. He then began his Postdoctoral research at the Graduate School of Life Science and Systems Engineering (Human Intelligence Systems), Kyushu Institute of Technology, where he investigated the potential of using carbon nanotubes for sensory and computational devices. Currently, he is working as an assistant professor at Waseda University, Graduate School of Information, Production and Systems. His research interests are the synthesis and characterization of nanomaterials, the design and application of flexible electronics and sensory devices, as well as wireless power transmission and remote sensing.

Kouki Kimizuka Kouki Kimizuka obtained his B.Sc from Fukuoka University, Department of Physical Science in 2021. He is currently pursuing a master's degree with the Kyushu Institute of Technology.

Gábor Méhes Dr. Méhes received Bachelor and Master of Science degrees in electronics from the Slovak University of Technology in Bratislava (Slovakia) in 2006 and 2008, respectively. After short internships at Omron Inc. (Japan) in UWB antenna engineering and Tampere University of Technology (Finland) in production engineering, he spent two years at Sony Slovakia as an LCD TV electrical engineer. He completed his doctoral degree at Kyushu University (Japan) in 2014 in organic photonics and electronics, followed by a researcher position at Fukuoka Industry, Science & Technology Foundation (Japan) in OLEDs. Between 2015 and 2020 he was a Marie Curie postdoctoral fellow and then a principal research engineer at Linköping University (Sweden) in organic bioelectronics, including a two-months stay at the Berkeley Lab in bacterial electronics in 2017. In 2020 Dr. Méhes moved back to Japan, where he was first a project assistant professor at Yamagata University in printed electronics and flexible hybrid electronics (FHE), and from 2022 is an assistant professor in bioelectronics at the Department of Information, Production and Systems, Waseda University. His research interests are mainly the application organic materials and devices for microbial electronics, sensing, energy harvesting and material conversion. Dr. Méhes has received several awards, including for poster and oral presentations, project proposal and as a journal reviewer.

Yuki Usami Yuki Usami received Ph.D degree in science from Osaka University in 2020. He is currently affiliated with Department of Human Intelligence Systems, Graduate school of Life Science and Systems Engineering, Kyushu Institute of Technology, Japan. He is currently working on the development of unconventional computing system composed of nanomaterials.

Yasuhiko Hayashi Yasuhiko Hayashi received the B.E., M.E., and D.E., degrees in electrical and computer engineering from the Nagoya Institute of Technology, Nagoya, Japan, in 1990, 1992, and 1999, respectively. From 1992 to 1996, he was engaged in research on semiconductor device modeling in Motorola Japan Ltd., Tokyo, Japan. He was appointed a Research Associate and an Associate Professor in the Department of Environmental Technology and Urban Planning at Nagoya Institute of Technology in 1999 and 2007, respectively, and then he was an Associate Professor in the Department of Frontier Materials at Nagoya Institute of Technology in 2008. He has been a full Professor in the Graduate School of Natural Science and Technology at Okayama University since October 2012. He has been a Visiting Professor at the Institute of Innovative Research, Tokyo Institute of Technology, since December 2016. He was appointed as Vice Executive Director for Research at Okayama University in April 2021.

Hirofumi Tanaka Hirofumi Tanaka (Senior Member, IEEE) received the Ph.D. degree in engineering from Osaka University in 1999. Professor Hirofumi Tanaka is a professor in Department of Human Intelligence Systems of Kyushu Institute of Technology (Kyutech), Japan. He is also a director of Research Center for Neuromorphic AI Hardware, Kyutech. His research interests are in Nanomaterials, Solid-state Chemistry and Physical Chemistry, to achieve Intelligence Emerging Nanosystems, and Neuromorphic AI Hardware Device based on nanomaterials especially carbon nanomaterials such as carbon nanotube and graphene nanoribbon with chemical dynamics.

Takeo Miyake Takeo Miyake, Ph.D., is a Professor of Graduate School of Information, Production and Systems at Waseda University. He graduated B.S. in Electrical Engineering in 2004, and then received the Ph.D. in Nanoscience and Nanoengineering in 2008 from Waseda University, working in Prof. Ohdomari's and Prof. Tanii's groups. He was selected for the young scientist program from the Japanese Society for the Promotion of Science. In 2009, he joined Tohoku University as an assistant professor in the Department of Bioengineering and Robotics, working with Prof. Nishizawa. He then moved to the US and joined the research group of Professor Marco Rolandi in Materials Science and Engineering at University of Washington (2014-2016) and in Electrical Engineering at University of California, Santa Cruz (2015-2016). In 2016, he started his independent academic career as an associate professor at Waseda University. He was promoted to a professor in 2021.